

EUR Research Information Portal

Sex-Specific Variances in Anatomy and Blood Flow of the Left Main Coronary Bifurcation

Published in:

IEEE Transactions on Biomedical Engineering

Publication status and date:

Published: 05/02/2025

DOI (link to publisher):

[10.1109/TBME.2025.3536161](https://doi.org/10.1109/TBME.2025.3536161)

Document Version

Publisher's PDF, also known as Version of record

Document License/Available under:

Article 25fa Dutch Copyright Act

Citation for the published version (APA):

Gharleghi, R., Zhang, M., Adikari, D., McGrath-Cadell, L., Graham, R. M., Wentzel, J. J., Webster, M., Ellis, C., Ooi, S. Y., & Beier, S. (2025). Sex-Specific Variances in Anatomy and Blood Flow of the Left Main Coronary Bifurcation: Implications for Coronary Artery Disease Risk. *IEEE Transactions on Biomedical Engineering*, 72(7), 2130-2137. <https://doi.org/10.1109/TBME.2025.3536161>

[Link to publication on the EUR Research Information Portal](#)

Terms and Conditions of Use

Except as permitted by the applicable copyright law, you may not reproduce or make this material available to any third party without the prior written permission from the copyright holder(s). Copyright law allows the following uses of this material without prior permission:






- you may download, save and print a copy of this material for your personal use only;
- you may share the EUR portal link to this material.

In case the material is published with an open access license (e.g. a Creative Commons (CC) license), other uses may be allowed. Please check the terms and conditions of the specific license.

Take-down policy

If you believe that this material infringes your copyright and/or any other intellectual property rights, you may request its removal by contacting us at the following email address: openaccess.library@eur.nl. Please provide us with all the relevant information, including the reasons why you believe any of your rights have been infringed. In case of a legitimate complaint, we will make the material inaccessible and/or remove it from the website.

Sex-Specific Variances in Anatomy and Blood Flow of the Left Main Coronary Bifurcation: Implications for Coronary Artery Disease Risk

Ramtin Gharleghi , Mingzi Zhang , Dona Adikari, Lucy McGrath-Cadell , Robert M. Graham , Jolanda J. Wentzel, Mark Webster, Chris Ellis, Sze-Yuan Ooi, and Susann Beier 

Abstract—Objective: Studies have shown marked sex disparities in Coronary Artery Diseases (CAD) epidemiology, yet the underlying mechanisms remain unclear. We explored the coronary anatomy and the resulting haemodynamics in patients with suspected but no significant CAD. Left Main (LM) bifurcations were 3D-reconstructed from 127 Computed Tomography Angiography images (42 males and 85 females, aged 38-81). **Methods:** Shape parameters including bifurcation angles, curvature, and diameters were measured, before solving the clinically relevant haemodynamic metrics. The severity and location of the vascular area exposed to adverse haemodynamics were compared between sexes. **Results:** Females were more likely than males to exhibit adversely low Time Averaged Endothelial Shear Stress (TAESS) along the inner wall of a bifurcation (16.8% vs. 10.7%). Males had a higher percentage of areas exposed to both adversely high Relative Residence Time (6.1% vs 4.2%, $p = 0.001$) and high Oscillatory Shear Index OSI (4.6% vs 2.3%, $p < 0.001$). However, the OSI values were generally small and should be interpreted cautiously. Males had larger arteries (M vs F, LM: 4.0 ± 0.5 mm vs 3.3 ± 0.6 mm, LAD: 3.6 ± 0.5 mm vs 3.0 ± 0.5 mm, LCX: 3.5 ± 0.5 mm vs 2.9 ± 0.6 mm), and females exhibited higher curvatures in all three branches (M

vs F, LM: 0.40 vs 0.46, LAD: 0.45 vs 0.51, LCx: 0.47 vs 0.55, $p < 0.001$). There was no difference in bifurcation angles. **Conclusion:** These differences may in part contribute to differences in CAD risk between sexes. **Significance:** This work facilitates a better understanding of sex differences in factors contributing to CAD, ultimately improving screening and therapeutic strategies particularly for women who currently have worse predictive outcomes.

Index Terms—Left main coronary artery, anatomical shape, haemodynamics, CTCA, sex disparity.

I. INTRODUCTION

SEX disparities in the incidence rates, clinical presentation, and management of CAD are well recognised. Despite a large and growing body of research into these disparities, women fared worse in most treatment metrics [2]. Previous scientific efforts towards rectifying these inequalities have predominantly focused on the differences in symptoms, physiology, and medical care provided [3]. Even though the link between atherosclerotic plaque development and coronary anatomy is well established in clinical [4], [5], and other literature [6], [7], [8], few studies have investigated sex differences in coronary anatomy and haemodynamics.

Established anatomical differences are that curvature/tortuosity [9] is higher in females [10], [11], [12], and that coronary artery diameters are larger in males even after correcting for body size [13], [14]. These findings raise the question: Could an anatomical difference between female and male CAD patients contribute to different haemodynamic profiles, leading to potential gender differences in the propensity to develop CAD?

Coronary anatomy is the predominant factor determining the local haemodynamics to which endothelial cells are exposed. Blood-flow-induced haemodynamic shear stresses on the inner arterial cell lining are a well-established driver of adverse biological cellular response [15]. Specifically, studies revealed that endothelial cells exposed to extremely low Endothelial Shear Stress (ESS, < 0.5 Pa) are prone to increased tissue growth factor secretion, promoting neointimal thickening and plaque progression [16], [17]. Moreover, frequent changes in the local ESS direction, quantified as the Oscillatory Shear Index (OSI, > 0.1) [18], were found to be associated with atheroma formation

Received 10 July 2024; revised 13 November 2024; accepted 16 January 2025. Date of publication 5 February 2025; date of current version 27 June 2025. This work was supported in part by the Auckland Academic Health Alliance (AAHA), in part by the Auckland Medical Research Foundation (AMRF), in part by the NSW Health Cardiovascular Research Capacity and NHMRC Ideas grant, in part by the Australian Government, and the computational cluster Katana through the research undertaken with the assistance of computational resources from the National Computational Infrastructure (NCI), and in part by the Research Technology Services at UNSW Sydney. (Correspondence author: Ramtin Gharleghi.)

Ramtin Gharleghi is with the School of Mechanical and Manufacturing Engineering, UNSW, Sydney, NSW 2033, Australia (e-mail: r.gharleghi@unsw.edu.au).

Mingzi Zhang and Susann Beier are with the School of Mechanical and Manufacturing Engineering, UNSW, Australia.

Dona Adikari and Sze-Yuan Ooi are with the Prince of Wales Clinical School of Medicine, Australia, and also with the Department of Cardiology, Prince of Wales Hospital, Australia.

Lucy McGrath-Cadell and Robert M. Graham are with the Molecular Cardiology and Biophysics Division, Victor Chang Cardiac Research Institute, Australia.

Jolanda J. Wentzel is with Erasmus, The Netherlands.

Mark Webster and Chris Ellis are with the Auckland City Hospital, New Zealand.

This article has supplementary downloadable material available at <https://doi.org/10.1109/TBME.2025.3536161>, provided by the authors.

Digital Object Identifier 10.1109/TBME.2025.3536161

[19]. The Relative Residence Time (RRT) has been proposed [20] to capture low and fluctuating ESS with $RRT > 4.17 \text{ Pa}^{-1}$ considered adverse [21], [22].

Despite the well-established understanding that anatomical characteristics induce clinically adverse haemodynamic endothelial cell response, the differences between males and females remain under-explored. Existing literature has reported smaller [13] and more curved [23] coronary arteries in women, as well as a larger inflow angle [24] between the LM and the bifurcation plane. These studies did not analyse the impact of these differences on the resulting haemodynamics. To our knowledge one study [25] considered haemodynamic differences, finding similar ESS between men and women, however this study only considered differences in coronary diameter. The haemodynamic differences resulting from different coronary anatomy is expected to affect both the risk and presentation of CAD [26], therefore necessitating more a detailed analysis of these haemodynamic conditions. Following our previous study in which we systematically analysed coronary anatomy in a large cohort of patients with suspected CAD [27], [28], we now explore the haemodynamic differences in males and females, thereby identifying potential sex-specific risk factors.

II. METHODS

A. Study Cohort

This study was approved by the local institutional ethics committees of the University of Auckland (Ref. 022961) and the University of New South Wales UNSW (Ref. HC190145), with informed written consent received from all participants. Patients were selected from those referred for imaging to investigate cardiovascular disease. We excluded patients with (i) reported atherosclerotic plaques or non-zero calcium score, (ii) CTCA images of insufficient quality for segmentation and computational modelling, for example, due to respiratory or motion artefacts, and (iii) patients with intermediate arteries as this study only concerns the left main bifurcation. A total of 127 CTCAs (42 men and 85 women), were included. The patient demographics are shown in Table I.

B. CTCA Acquisition Protocol

All patients underwent CTCA scans using a 64-slice CT scanner (GE LightSpeed, USA) with retrospective ECG-gated acquisition. The contrast-enhanced images were obtained with intravenously administered 60-80 mL of a non-ionic medium (Omnipaque 350, GE Healthcare, USA). Where necessary, beta-blockers were administered to reduce heart rate to around 60 beats per minute. Images were taken at the end-diastolic phase for each patient.

C. Vessel Reconstruction and Shape Analysis

The coronary arteries were segmented and reconstructed from the patients' CTCA images, as previously reported [28]. OsiriX (v4.1.2) was used for semi-automatic segmentation of the arteries, producing a triangulated surface mesh. The four heart chambers were segmented using a deep learning model and

TABLE I
SUMMARY OF THE 127 PATIENT DEMOGRAPHICS BY SEX

	Male	Female
Ethnicity	Caucasian 86%	Caucasian 88%
	Other 14%	Other 12%
Weight [kg]*	88.4 ± 11.4	72.7 ± 12.9
Height [m]*	1.78 ± 0.075	1.63 ± 0.067
Systolic Blood Pressure [mmHg]	132.9 ± 16.4	131 ± 26.2
Diastolic Blood Pressure [mmHg]*	84.4 ± 10.5	77.3 ± 14.1
Body Mass Index (BMI)	27.8 ± 3.55	27.2 ± 4.72
Smoking History (count)	26.1% (11)	35.3% (30)
Hypertension (count)	28.6% (12)	28.2% (24)
Diabetes (count)	0% (0)	3.5% (3)
Age [years]*	53.3 ± 6.18	57.2 ± 7.67

An asterisk indicates that the mean values were significantly different between groups.

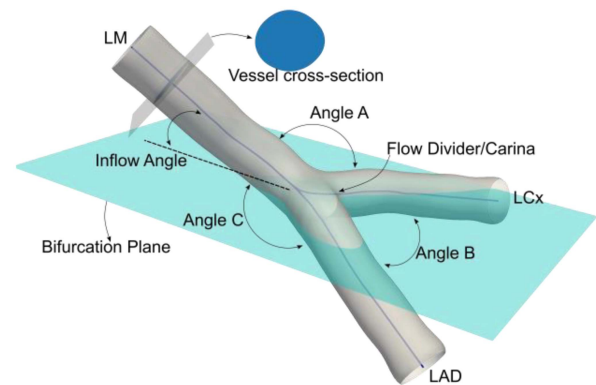


Fig. 1. Left main coronary shape definition: Anatomical parameters defined for the coronary left main bifurcation comprised of the left main (LM), left anterior descending (LAD), and left circumflex (LCx) branch.

heart size was calculated as the sum of the volume of the four chambers. The left main bifurcation was extracted from the coronary tree with a maximum length of 10mm for the LM and daughter branches. The bifurcation was smoothed using a Taubin filter [29] with a passband of 0.03 and 30 iterations. The shape parameters were measured using an in-house python script and included the inflow angle, and bifurcation angles A, B and C as defined by the European Bifurcation Club [30] (Fig. 1).

Angles were measured between the average tangent vectors for the first 5 mm of the vessels. The inflow angle is the angle between LM and the bifurcation plane [28], defined as the best-fit plane containing the first 5 mm of LAD and LCx centrelines. The median diameter for each vessel, corresponding to the diameter of a circle with equivalent cross-sectional area, was calculated over the 10 mm segment comprised of intervals with 0.01 mm spacing. As the change in vessel diameter along the vessel length is relatively small (standard deviation of 0.1 mm for calculated diameters), the median should be a representative measure. Finet's ratio (FR) is defined as the ratio of the LM diameter

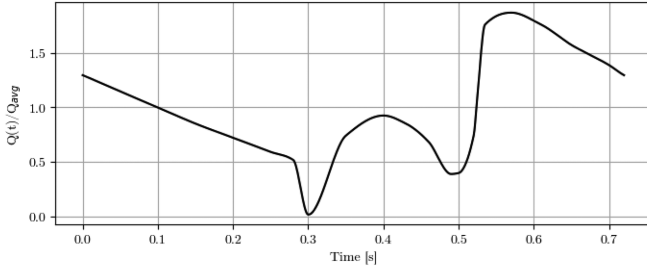


Fig. 2. Variation of inflow rate over the cardiac cycle. This curve has an average value of 1.0 over the cardiac cycle, such that multiplying by the average flow rate calculated from [1] results in the correct average flow rate.

over the sum of the daughter branch diameters ($\frac{d_{LM}}{d_{LAD}+d_{LCx}}$, [30], [31]). We calculated the mean curvature of all branches, which was demonstrated as a superior tortuosity measure than the commonly used tortuosity index [9].

D. Haemodynamic Simulation

Following a sensitivity test, we generated unstructured tetrahedral meshes using TetGen [32] with an average of 2 million elements per bifurcation (average element volume of $1.77 \cdot 10^{-4} \text{ mm}^3 \pm 1.43 \cdot 10^{-4} \text{ mm}^3$). The timestep size was 0.002 seconds. The mesh was imported into ANSYS CFX v19.3 (Canonsburg, PA) to resolve the haemodynamic metrics. A generic flowrate waveform (Fig. 2, [33]) was prescribed at the extended inlet, scaled based on the relationship (flowrate in $\text{m}^3/\text{s} = 1.43 \cdot d_{LM}^{2.55}$, where d is the vessel diameter in meters) as proposed by Giessen et al. [1]. This resulted in an average flowrate of $52 \pm 23 \text{ ml/min}$ (male: $69 \pm 22.6 \text{ ml/min}$, female: $44 \pm 18.8 \text{ ml/min}$). A plug flow profile was applied as suitable to simulate a region close to the coronary ostia. A constant reference pressure of 0 Pa was specified at the outlets appropriate for non-diseased vessels, allowing for a computationally stable solution and validated *in vitro* [34]. The vessels were modelled as rigid in line with existing literature [35]. A laminar fluid model was prescribed, resulting in average Reynolds numbers of 600. We utilized the non-Newtonian Carreau-Yasuda [36] model, with parameters $\mu_0 = 0.16 \text{ Pa}\cdot\text{s}$, $\mu_\infty = 0.0035 \text{ Pa}\cdot\text{s}$, $\lambda = 8.2 \text{ s}$, $b = 1.23$, $a = 0.64$. The simulations were run on the Katana computing cluster [37]. The RMS Courant number was 2.34, with the maximum over all cases and mesh nodes reaching up to 57. We note that as ANSYS CFX is an implicit solver, low Courant numbers are not required for stability [38], [39]. Sensitivity analysis did not show a significant change in results with lower timesteps.

E. Haemodynamic Conditions

Following previous studies [8], [40], we considered the local haemodynamic environment adverse to the endothelial cells if coronary arteries are exposed to (i) Low Time Averaged Endothelial Shear Stress (also commonly referred to as Wall Shear Stress, WSS, in previous literature), i.e., TAESS $< 0.5 \text{ Pa}$, (ii) High Oscillatory Shear Index, i.e., OSI > 0.1 , or (iii) high Relative Residence Time, i.e., RRT $> 4.17 \text{ Pa}^{-1}$. We extracted the ESS vector τ_w from the fourth cardiac cycle to minimise

the transient start-up effects. The TAESS, OSI, and RRT were then derived as follows:

$$\text{TAESS} = \frac{1}{T} \int_0^T |\tau_w| dt \quad (1)$$

$$\text{OSI} = \frac{1}{2} \left(1 - \frac{\int_0^T |\tau_w| dt}{\int_0^T |\tau_w| dt} \right) \quad (2)$$

$$\text{RRT} = \frac{1}{(1-2 \cdot \text{OSI}) \cdot \text{TAESS}} \quad (3)$$

where T is the cardiac cycle period. In addition to analysing these measurements' normalised adverse area size, we also studied their respective locations within the left main branches. The percentage of the vessel area exposed to low TAESS, high OSI, and high RRT are referred to as low TAESS%, high OSI%, and high RRT%, respectively.

F. Statistical Modelling

Continuous variables describing the study cohort are presented as mean \pm Standard Deviation. Nominal variables are presented as numbers and percentages. Sex was determined as significant using a type-I Analysis of Variance (ANOVA) test before using a Welch's t-test to determine the difference of means for each shape parameter, i.e., diameter, curvature, bifurcation angles A, B, C and Inflow. Welch's t-test was used for statistical comparisons. It is important to note that this is a robust method for the different variances of the two groups [41], and is also robust against normality violations [42]. Body size is a confounding factor for arterial diameter [43], which was accounted for using both the Body Surface Area (BSA), and Body Mass Index (BMI) in a multivariate linear model. The results were analysed using python and its statsmodels package (v0.11.0). A standard linear model assumption was used with $p < 0.05$ considered statistically significant. Statistically significant differences are marked with an asterisk *.

III. RESULTS

A. Geometric Differences Between Males and Females

Sex-specific differences in the curvature and diameter of all branch vessels were found, see Table II. Specifically, diameters of the coronary arteries were larger (all $p < 0.001^*$) in males (LM: 4.02 ± 0.52 , LAD: 3.62 ± 0.50 , and LCx: 3.51 ± 0.53) than in females (LM: 3.33 ± 0.61 , LAD: 3.01 ± 0.50 , and LCx: 2.88 ± 0.57), as shown in Fig. 3. The differences in vessel diameter remained statistically significant even after adjusting for BMI ($p < 0.001^*$ for all branches), BSA ($p = 0.001^*$ for all branches), and heart volume ($p = 0.02^*$ for all branches) by including these in a multivariate linear model.

The mean curvature was significantly higher in female patients for all branches (M vs F, LM: 0.40 ± 0.08 vs 0.46 ± 0.12 , LAD: 0.45 ± 0.07 vs 0.51 ± 0.11 , LCX: 0.47 ± 0.08 vs 0.55 ± 0.13 , $p = 0.001^*$). Curvature and diameter sex differences are visualised in Fig. 4. Of the bifurcation angles, only the inflow angle varied between males and females, with females showing slightly larger acute inflow angles than males (M vs F: $12.9^\circ \pm 11.2^\circ$ vs $18.5^\circ \pm 15.9^\circ$, $p = 0.025^*$). No statistical

TABLE II
ANATOMICAL CHARACTERISTICS BY SEX AND OVERALL

Feature	Male	Female	p-value	Difference	
				M-F	95% CI
Angle A [°]	125.4 ± 17.1	122.9 ± 21.2	0.516	2.47	[-4.54 9.47]
Angle B [°]	81.9 ± 18.6	77.9 ± 18.6	0.267	3.96	[-3.10 11.0]
Angle C [°]	146.7 ± 10.7	150.1 ± 21.7	0.244	-3.39	[-9.12 2.34]
Inflow Angle [°]	12.9 ± 11.2	18.5 ± 15.9	0.025*	-5.57	[-10.4 -0.70]
LM diameter [mm]	4.02 ± 0.52	3.33 ± 0.61	<0.001*	0.69	[0.48 0.90]
LAD diameter [mm]	3.62 ± 0.50	3.01 ± 0.50	<0.001*	0.61	[0.42 0.79]
LCx diameter [mm]	3.51 ± 0.53	2.88 ± 0.57	<0.001*	0.63	[0.42 0.84]
LM curvature [mm ⁻¹]	0.40 ± 0.08	0.46 ± 0.12	0.001*	-0.062	[-0.01 -0.03]
LAD curvature [mm ⁻¹]	0.45 ± 0.07	0.51 ± 0.11	0.001*	-0.063	[-0.10 -0.03]
LCx curvature [mm ⁻¹]	0.47 ± 0.08	0.55 ± 0.13	0.001*	-0.072	[-0.11 -0.03]
Finet's ratio	0.57 ± 0.02	0.57 ± 0.04	0.984	0.0001	[-0.01 0.01]

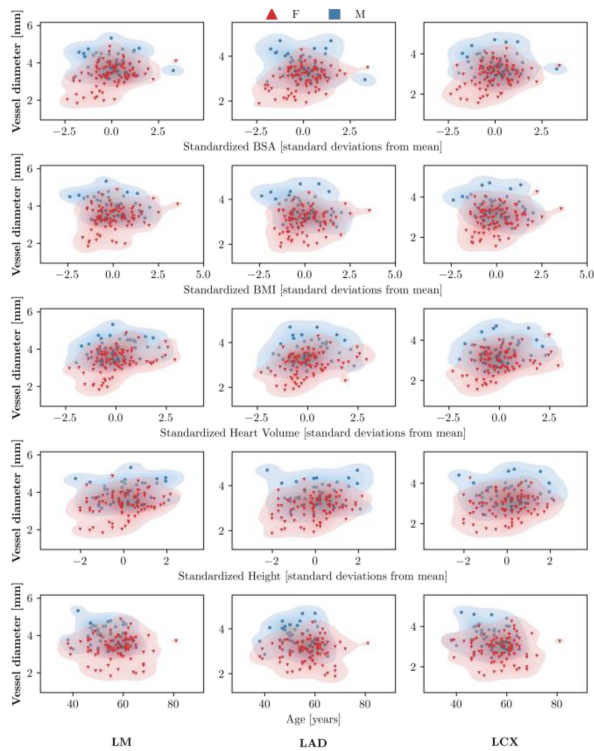


Fig. 3. Distribution of left main branch diameters by sex: Vessel diameter of Left Main (LM), Left Anterior Descending (LAD), and Left Circumflex (LCx, left to right) for females (red) and males (blue) over suspected confounding factors, i.e., standardized ± 2 SD.

difference in the Finet's Ratio was found. All results are listed in Table II.

B. Haemodynamic Differences

Whilst the overall percentage of vascular surface exposure to low TAESS was similar between males and females (M 26.8% vs F 25.0%, $p = 0.274$), an interesting difference in spatial

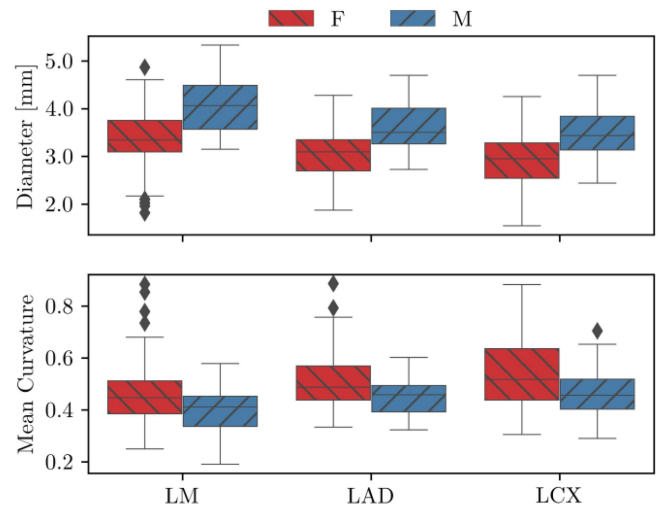


Fig. 4. Sex differences in left main curvature and branch diameters: Left main branch diameters (top), and mean curvature (bottom) for females (red) and males (blue) in the Left Main (LM), Left Anterior Descending (LAD), and Left Circumflex (LCx). The diameter ($p < 0.001^*$), and mean curvature ($p < 0.01^*$).

distributions appeared whereby low TAESS% was shifted towards the flow divider and inner vessel walls in female patients. Specifically, when defining the inner and outer vessel regions (using 90°, 135°, or 180° wedges centred along the bifurcation plane (Fig. 5) the percentage of the inner wall exposed to low TAESS was significantly higher in females (M 10.6% vs F 16.8%, $p = 0.004^*$). Similarly, for the outer walls, low TAESS% was higher in males (M 59.9% vs F 47.8%, $p < 0.001^*$). See the Supplementary Material for details.

Differences in diameter ($R^2 = 0.46$, $p < 0.001^*$) and mean curvature between the two groups ($R^2 = 0.37$, $p < 0.001^*$) appear to drive this regional shift in low TAESS% when using linear regression models between the shape features and the difference in low TAESS% for the inner/outer wall distribution. Specifically, smaller vessel diameters and higher overall bifurcation curvature shift adverse low TAESS% distribution towards the inner proximal daughter branch vessel walls.

Men showed higher adverse values in both high OSI% (M 4.57% vs F 2.34%, $p < 0.001^*$), and high RRT% (M 6.6% vs F 4.24%, $p = 0.005^*$), which infers higher disturbed and oscillatory flow conditions in males compared to females (see Table III and Fig. 6).

All reported differences in high OSI%, high RRT%, and spatial distribution of low TAESS% remained statistically significant when adjusted for age, height, BMI, BSA, heart volume, smoking history, and hypertension in a multivariate linear model. Fig. 7 shows the distribution of haemodynamic variables against these factors.

IV. DISCUSSION

This work quantifies the differences between male and female patients undergoing CTCA imaging for suspected CAD with no significant coronary artery stenosis, analysing anatomical and haemodynamic metrics. It should be noted that this study uses

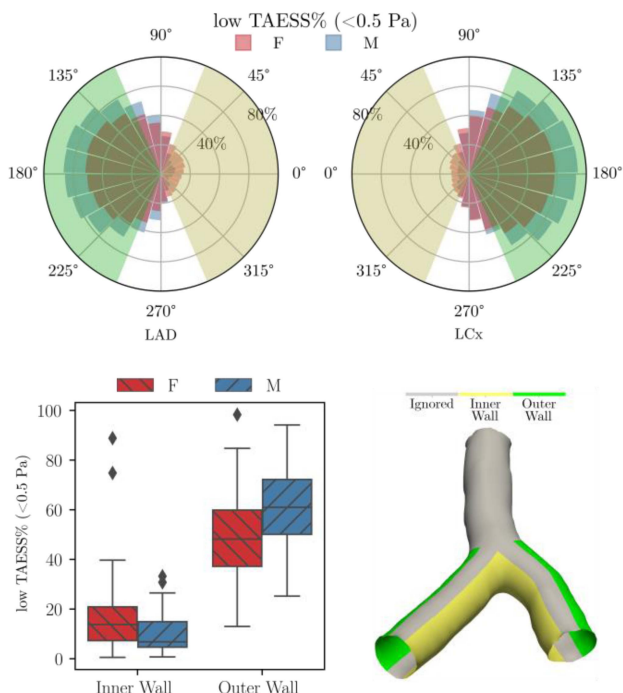


Fig. 5. Radial difference by sex in low TAESS% proximal to the left main carina: Percentage of low TAESS for females (red) and males (blue) based on radial location for both the LAD (top left) and LCx (top right) daughter branches. Differences in the spatial distribution of low TAESS% are shown as a box plot (bottom left) for the inner (yellow) and outer (green) wall regions (bottom right), again for females (red) and males (blue), here visualised for a 135° region (bottom right)). As shown in the Supplementary Material, the choice of region size did not have a significant effect.

TABLE III

HAEMODYNAMIC DIFFERENCES OF LOW TAESS% OVERALL, AT THE INNER AND OUTER WALL, HIGH OSI%, HIGH RRT%, AND MEAN HAEMODYNAMIC METRICS BETWEEN SUSPECTED CAD MALES AND FEMALES LEFT MAIN CORONARY BIFURCATIONS WITHOUT SIGNIFICANT STENOSIS

Metric	Male	Female	p-value	Difference	
				M-F	95% CI
low TAESS%	26.83 ± 8.00	25.01 ± 9.90	0.274	1.818	[-1.46 5.10]
low TAESS%, Inner wall	10.71 ± 8.76	16.78 ± 14.47	0.004*	-6.07	[-10.21 -1.93]
low TAESS%, Outer wall	59.88 ± 17.21	47.87 ± 16.15	<0.001*	12.01	[5.61 18.42]
high OSI%	4.57 ± 2.80	2.35 ± 1.68	<0.001*	2.22	[1.27 3.18]
high RRT%	6.06 ± 3.56	4.24 ± 2.57	0.005*	1.82	[0.58 3.07]
Mean TAESS	0.73 ± 0.068	0.741 ± 0.077	0.435	-0.011	[-0.038 0.016]
Mean OSI	0.027 ± 0.008	0.018 ± 0.006	<0.001*	0.008	[0.005 0.011]
Mean RRT	2.059 ± 0.403	1.854 ± 0.288	0.005*	0.204	[0.063 0.345]

retrospective CTCA data collected when assessing patients for coronary artery disease. While it would be ideal to recruit a cohort tailored to investigating these findings, ethical concerns make it difficult to recruit a large sample. We have employed rigorous statistical adjustments to mitigate potential confounding effects, although some potentially relevant characteristics, such as blood biomarker data, are unavailable. Additionally, we

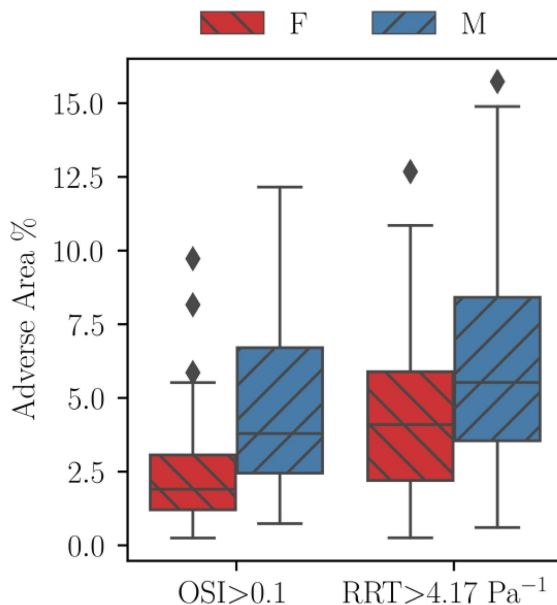


Fig. 6. Sex differences in left main OSI and RRT: Differences in normalised percentage vessel area coverage of adversely high Oscillatory Shear Index (left) and Relative Resident Time (right) haemodynamic metrics in females (red) and males (blue).

cannot account for effects of thorax height and volume here, however as these features are strongly influenced by sex [44], it is unlikely they would have a strong confounding effect. From a fluid dynamics perspective, the inflow profile was previously found to have no significant effect on flow [45], and only upstream geometry would be relevant, which we accounted for here. Taking these considerations into account, our findings have the potential to improve understanding of plaque locations and thereby sex-specific considerations for PCI procedures. It opens a new consideration in the field, previously hindered due to imaging modality constraints and a lack of large enough relevant cohort sizes. However, further testing and validation remains necessary to confirm the potential clinical relevance of our results

Shape characteristics, such as the average vessel diameter [46], [47] and curvature [22], [48] of coronary arteries, have been established as potential anatomical risk markers owing to their demonstrated effect in generating local haemodynamics with clinically adverse associations. However, it should be noted that some or many of these characteristics may have interdependent effects, as previously demonstrated for the left main bifurcation angle showcasing that only in combination with other anatomical characteristics certain bifurcation angles generate adverse haemodynamics [49]. Similarly, the differences tested may be further affected and compounded by other variables outside the realms of the current study and thus have to be interpreted in its findings as such.

We found vessel diameters to be larger in males compared to females, even after adjusting for age, height, BMI, BSA, and heart volume, which is in line with previously reported results [13]. Additionally, it should be noted that our prior work [24] reported differences in Angle B between males and females

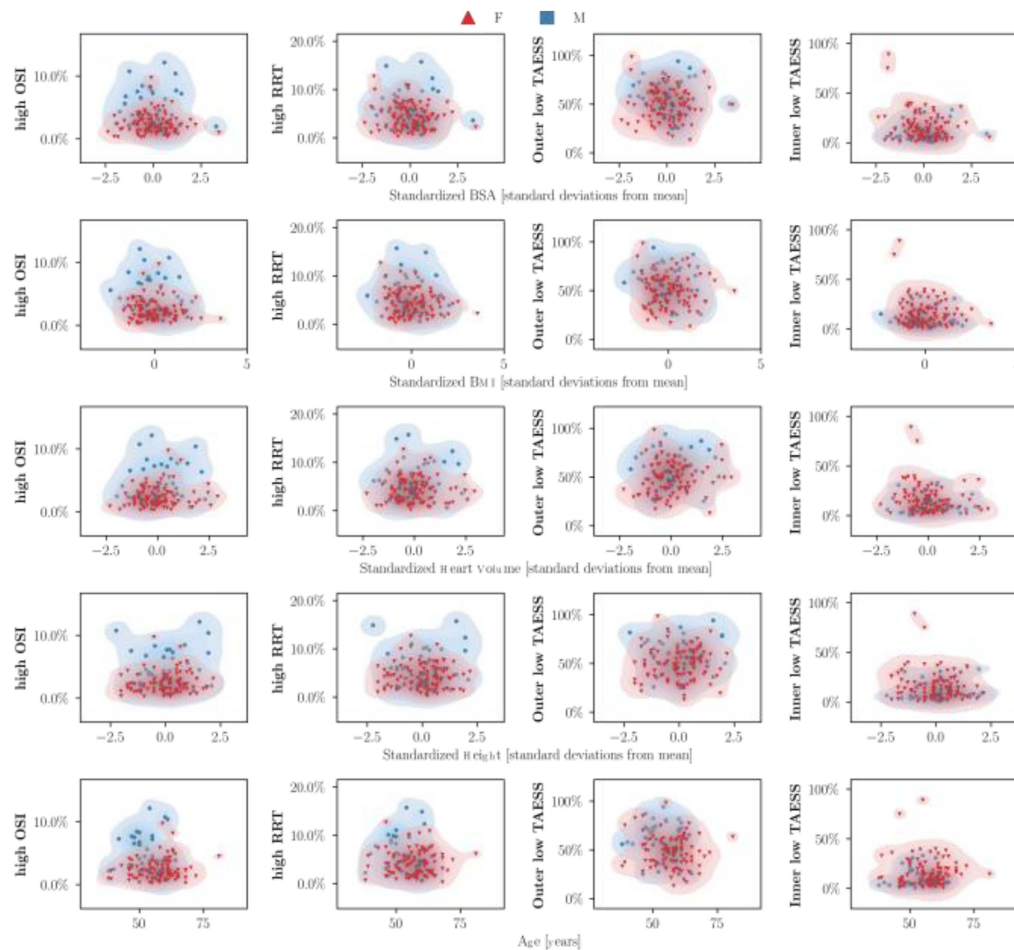


Fig. 7. Distribution of haemodynamic metrics, i.e., high OSI, high RRT, outer low TAESS, inner low TAESS (left to right) by sex for females (red) and males (blue) over suspected confounding factors, i.e., standardized \pm 2SD Body Surface Area (BSA), Body Mass Index (BMI), heart volume, height, and age (top to bottom).

when cases with intermediate arteries were included. Here, after excluding intermediate arteries, no statistically significant difference in Angle B was found.

Tortuosity is well known to be greater in females than males [14], [23], [50]. While these studies quantify tortuosity using the tortuosity index, we have previously shown that tortuosity index is not reliable and mean curvature is a better measure of tortuosity [9]. To our knowledge other groups have not reported gender differences using the mean curvature metric, however our results are in alignment with the literature using tortuosity index. Increased arterial tortuosity is associated with both atherosclerotic coronary disease and non-atherosclerotic Spontaneous Coronary Artery Dissection (SCAD), a less common condition presenting at a younger age and affecting women far more often than men [51]. It has been proposed that increased arterial curvature would cause an increase in shear stress, which may weaken the vascular wall and ultimately lead to SCAD [11], [23]. Recent work also linked SCAD to additional measures describing regional extreme TAESS zones [52], [53]. Previous studies found sex-specific differences in plaque size, and also differences in ESS when stratified by age [25]. However, this study did not consider the radial position of plaques, and thus, a direct comparison is difficult. Further, our cohort did not

allow a meaningful analysis in terms of age, although it should be noted that the mean age differed statistically between the two groups, with males being approximately 4 years younger than females. Previous studies of carotid arteries [54] did not show a difference in the radial distribution of plaques between male and female patients. To our knowledge, no previous study has explored sex-specific radial haemodynamics in coronaries before our work presented here.

Similarly, the effect of the significant sex-specific difference in inflow angle and diameter, as found here, their haemodynamic impact, and, thus, their potential clinical association has not been explored or reported before and warrants future studies.

In women, coronary artery disease often manifests as a non-obstructive disorder [55], and is more challenging to diagnose, indicating the need for sex-specific patient care [56]. Non-obstructive CAD correlates to severe endothelial dysfunction through low ESS [57]. Whilst low TAESS% was not different between males and females, the spatial distribution differed. This may result in different locations of plaque development, and may also affect its progression by inducing different haemodynamics. This would not be observable by today's standard imaging modalities, which are usually portrayed longitudinally, and too limited in resolution to observe nuanced axial differences.

We also observed higher oscillatory conditions in males, a predictor of neointimal thickening, which is the initial stage of atherosclerosis development [58]. This may indicate that males are haemodynamically more prone to obstructive lesions compared to females. Since the males in this cohort also had no significant stenosis, an equivalent study in males versus females should be undertaken in those with obstructive disease to investigate this further, with addition of other relevant predictors such as blood biomarkers, medical histories, and co-morbidities. While we can not validate whether these findings predict disease development in our cohort as only patients without disease are included, low and oscillatory shear stress are well-known risk factors for CAD [4], [5], [59].

The inclusion of sex as a CAD risk factor is clinically relevant. Males develop atherosclerotic CAD at a younger age than females, and females are more prone to non-obstructive CAD and non-atherosclerotic coronary artery disease, such as SCAD. Hence, disease risk stratification must be viewed differently in the context of the patient's sex regarding their clinical diagnosis, management, and outcomes [60]. This difference in haemodynamics between male and female cases represents a promising area for further research given the well-established differences in CAD development and presentation based on sex [2], [60], potentially impacting risk management and interventions due to the expected difference in plaque locations. There have not been any prospective longitudinal studies on the implications of low TAESS% on the development of CAD, which would inform the understanding of the onset and progression of atherosclerosis. As mentioned, certain conditions like SCAD may be due, at least in part, to greater vessel curvature in females. Hypertensive women have a high risk of non-obstructive CAD. Moreover, hypertension often starts around menopausal in females, and even mild hypertension (140/90 mmHg) causes endothelial dysfunction, leading to disease [61].

The new insights from evaluating potential geometric risk factors and their local haemodynamic characteristics may be critical to understanding CAD risk factors better in both sexes. Significantly, women may benefit from this due to commonly atypical and under-recognised presentations. Improved prediction and early prevention may be the key to improving outcomes.

Future studies should include obstructive and non-obstructive disease cohorts, and may also elaborate further on other compounding factors, such as hypertension, diabetes, and pre- and post-menopausal effects, to inform longitudinal risk stratification effective in both sexes. Additionally, in this study we utilize the same rheological model for both male and female cases, whereas it is expected that different haematocrit levels will cause differences in blood viscosity between male and female cases [62].

V. CONCLUSION

This work has shown significant differences in the anatomical features and resulting haemodynamic profiles of LM bifurcations in males and females with suspected CAD but non-significant stenosis. Namely, low TAESS was more commonly found in the inner proximal bifurcation walls in females and

outer walls in males. Males showed a significantly higher percentage of high OSI, likely due to larger vessel size, fewer curvatures and more accurate inflow angles than females. These findings may have future implications for our understanding of sex-specific CAD development and inform more personalised assessment and treatment considerations. Further studies are warranted to investigate underlying mechanisms that may lead to sex-specific screening and therapeutic strategies and, thus, improved outcomes for women and men with CAD.

ACKNOWLEDGEMENT

The authors would like to thank Intra for assistance in collecting the dataset.

REFERENCES

- [1] A. G. van der Giessen et al., "The influence of boundary conditions on wall shear stress distribution in patients specific coronary trees," *J. Biomech.*, vol. 44, no. 6, pp. 1089–1095, 2011.
- [2] G. Mnatzaganian et al., "Sex disparities in the assessment and outcomes of chest pain presentations in emergency departments," *Heart (Brit. Cardiac Soc.)*, vol. 106, no. 2, pp. 111–118, 2020.
- [3] P. Presbitero and A. Carcagn, "Gender differences in the outcome of interventional cardiac procedures," *Italian Heart J.*, vol. 4, pp. 522–527, 2003.
- [4] P. H. Stone et al., "Effect of endothelial shear stress on the progression of coronary artery disease, vascular remodeling, and in-stent restenosis in humans: In vivo 6-month follow-up study," *Circulation*, vol. 108, no. 4, pp. 438–444, 2003.
- [5] M. A. Gimbrone Jr. and G. Garca-Cardea, "Endothelial cell dysfunction and the pathobiology of atherosclerosis," *Circulation Res.*, vol. 118, no. 4, pp. 620–636, 2016.
- [6] M. Zhou et al., "Wall shear stress and its role in atherosclerosis," *Front. Cardiovasc. Med.*, vol. 10, 2023, Art. no. 1083547.
- [7] P. Eshtehardi et al., "Association of coronary wall shear stress with atherosclerotic plaque burden, composition, and distribution in patients with coronary artery disease," *J. Amer. Heart Assoc.*, vol. 1, no. 4, 2012, Art. no. e002543.
- [8] U. Morbiducci et al., "Atherosclerosis at arterial bifurcations: Evidence for the role of haemodynamics and geometry," *J. Thromb. Haemostasis*, vol. 115, no. 3, pp. 484–492, Mar. 2016.
- [9] V. Kashyap et al., "Accuracy of vascular tortuosity measures using computational modelling," *Sci. Rep.*, vol. 12, no. 1, 2022, Art. no. 865.
- [10] S. Sharma et al., "Risk factors, imaging findings, and sex differences in spontaneous coronary artery dissection," *Amer. J. Cardiol.*, vol. 123, no. 11, pp. 1783–1787, 2019.
- [11] S. Cioric et al., "Arterial tortuosity," *J. Amer. Heart Assoc.*, vol. 73, no. 5, pp. 951–960, 2019.
- [12] F. Kahe et al., "Coronary artery tortuosity: A narrative review," *Coronary Artery Dis.*, vol. 31, no. 2, pp. 187–192, 2020.
- [13] I. Ilayperuma, B. G. Nanayakkara, and K. N. Palahepitiya, "Sexual differences in the diameter of coronary arteries in an adult Sri Lankan population," *Int. J. Morphol.*, vol. 29, no. 4, pp. 1444–1448, 2011.
- [14] J. Chiha et al., "Gender differences in the prevalence of coronary artery tortuosity and its association with coronary artery disease," *IJC Heart Vasculture*, vol. 14, pp. 23–27, 2017.
- [15] A. B. Fisher et al., "Endothelial cellular response to altered shear stress," *Amer. J. Physiol.-Lung Cellular Mol. Physiol.*, vol. 281, no. 3, pp. L529–L533, 2001.
- [16] E. Cecchi et al., "Role of hemodynamic shear stress in cardiovascular disease," *Atherosclerosis*, vol. 214, no. 2, pp. 249–256, 2011.
- [17] S. L. Meyerson et al., "The effects of extremely low shear stress on cellular proliferation and neointimal thickening in the failing bypass graft," *J. Vasc. Surg.*, vol. 34, no. 1, pp. 90–97, 2001.
- [18] X. Xie et al., "Computation of hemodynamics in tortuous left coronary artery: A morphological parametric study," *J. Biomech. Eng.*, vol. 136, no. 10, 2014, Art. no. 101006.
- [19] D. N. Ku et al., "Pulsatile flow and atherosclerosis in the human carotid bifurcation. Positive correlation between plaque location and low oscillating shear stress," *Arteriosclerosis*, vol. 5, no. 3, pp. 293–302, May 1985.

- [20] H. A. Himburg et al., "Spatial comparison between wall shear stress measures and porcine arterial endothelial permeability," *Amer. J. Physiol.-Heart Circulatory Physiol.*, vol. 286, no. 5, pp. H1916–H1922, 2004.
- [21] M. F. Rabbi, F. S. Laboni, and M. T. Arafat, "Computational analysis of the coronary artery hemodynamics with different anatomical variations," *Inform. Med. Unlocked*, vol. 19, 2020, Art. no. 100314.
- [22] C. Chiastra et al., "Healthy and diseased coronary bifurcation geometries influence near-wall and intravascular flow: A computational exploration of the hemodynamic risk," *J. Biomech.*, vol. 58, pp. 79–88, Jun. 2017.
- [23] M. F. Eleid et al., "Coronary artery tortuosity in spontaneous Coronary artery dissection: Angiographic characteristics and clinical implications," *Circulation. Cardiovasc. Interv.*, vol. 7, no. 5, pp. 656–662, 2014.
- [24] P. Medrano-Gracia et al., "A computational atlas of normal coronary artery anatomy," *EuroIntervention*, vol. 12, no. 7, pp. 845–854, Sep. 2016.
- [25] J. J. Wentzel et al., "Sex-related differences in plaque characteristics and endothelial shear stress related plaque-progression in human coronary arteries," *Atherosclerosis*, vol. 342, pp. 9–18, 2022.
- [26] V. R. Taqueti, "Sex differences in the coronary system," *Sex-Specific Anal. Cardiovasc. Function*, vol. 1065, pp. 257–278, 2018, doi: [10.1007/978-3-319-77932-4_17](https://doi.org/10.1007/978-3-319-77932-4_17).
- [27] P. Medrano-Gracia et al., "Construction of a coronary atlas from CT Angiography," in *Proc. Med. Image Comput. Comput. Assist. Intervention: 17th Int. Conf.*, 2014, pp. 513–520, doi: [10.1007/978-3-319-10470-6_64](https://doi.org/10.1007/978-3-319-10470-6_64).
- [28] P. Medrano-Gracia et al., "A study of coronary bifurcation shape in a normal population," *J. Cardiovasc. Transl. Res.*, vol. 10, pp. 82–90, 2016.
- [29] G. Taubin, "Curve and surface smoothing without shrinkage," in *Proc. IEEE Int. Conf. Comput. Vis.*, 1995, pp. 852–857.
- [30] J. A. Ormiston et al., "Bench testing and coronary artery bifurcations: A consensus document from the European Bifurcation Club," *EuroIntervention*, vol. 13, no. 15, pp. e1794–e1803, 2018.
- [31] G. Finet et al., "Fractal geometry of arterial coronary bifurcations: A quantitative coronary angiography and intravascular ultrasound analysis," *EuroIntervention*, vol. 3, no. 4, pp. 490–498, 2008.
- [32] H. Si, "TetGen, a Delaunay-based quality tetrahedral mesh generator," *Assoc. Comput. Machinery Trans. Math. Softw.*, vol. 41, no. 2, 2015, Art. no. 11.
- [33] W. W. Nichols et al., "The Coronary Circulation," in *McDonald's Blood Flow in Arteries: Theoretical, Experimental and Clinical Principles*, Boca Raton, FL, USA: CRC Press, 2011, pp. 375–396.
- [34] S. Beier et al., "Dynamically scaled phantom phase contrast MRI compared to true-scale computational modeling of coronary artery flow," *J. Magn. Reson. Imag.*, vol. 44, no. 4, pp. 983–992, 2016.
- [35] P. Eslami et al., "Effect of wall elasticity on hemodynamics and wall shear stress in patient-specific simulations in the coronary arteries," *J. Biomech. Eng.*, vol. 142, no. 2, 2020, Art. no. 024503.
- [36] A. Razavi, E. Shirani, and M. R. Sadeghi, "Numerical simulation of blood pulsatile flow in a stenosed carotid artery using different rheological models," *J. Biomech.*, vol. 44, no. 11, pp. 2021–2030, Jul. 2011.
- [37] "Katana," PVC (Research Infrastructure), UNSW Sydney, Kensington, Australia, 2010, doi: [10.26190/669X-A286](https://doi.org/10.26190/669X-A286).
- [38] S. Qin et al., "Numerical simulation of blood flows in patient-specific abdominal aorta with primary organs," *Biomech. Model. Mechanobiology*, vol. 20, pp. 909–924, 2021.
- [39] F. Tan et al., "Analysis of flow patterns in a patient-specific thoracic aortic aneurysm model," *Comput. Struct.*, vol. 87, no. 11/12, pp. 680–690, 2009.
- [40] A. M. Malek, "Hemodynamic shear stress and its role in atherosclerosis," *JAMA*, vol. 282, no. 21, Dec. 1999, Art. no. 2035.
- [41] B. Derrick, D. Toher, and P. White, "Why Welch's test is type I error robust," *Quantitative Methods Psychol.*, vol. 12, no. 1, pp. 30–38, 2016.
- [42] M. Delacre, D. Lakens, and C. Leys, "Why psychologists should by default use Welch's t-test instead of Student's t-test," *Int. Rev. Social Psychol.*, vol. 30, no. 1, pp. 92–101, 2017.
- [43] M. H. Friedman et al., "Arterial geometry affects hemodynamics. A potential risk factor for atherosclerosis," *Atherosclerosis*, vol. 46, no. 2, pp. 225–231, 1983.
- [44] F. Bellemare, A. Jeanneret, and J. Couture, "Sex differences in thoracic dimensions and configuration," *Amer. J. Respir. Crit. Care Med.*, vol. 168, no. 3, pp. 305–312, 2003.
- [45] J. G. Myers et al., "Factors influencing blood flow patterns in the human right coronary artery," *Ann. Biomed. Eng.*, vol. 29, no. 2, pp. 109–120, 2001.
- [46] Y. Huo et al., "Which diameter and angle rule provides optimal flow patterns in a coronary bifurcation?," *J. Biomech.*, vol. 45, no. 7, pp. 1273–1279, 2012.
- [47] N. A. Papakonstantinou et al., "Sex differentiation with regard to coronary artery disease," *J. Cardiol.*, vol. 62, no. 1, pp. 4–11, 2013.
- [48] C. Shen et al., "Secondary flow in bifurcations—important effects of curvature, bifurcation angle and stents," *J. Biomech.*, vol. 129, 2021, Art. no. 110755.
- [49] S. Beier et al., "Impact of bifurcation angle and other anatomical characteristics on blood flow A computational study of non-stented and stented coronary arteries," *J. Biomech.*, vol. 49, no. 9, pp. 1570–1582, Jun. 2016.
- [50] Y. Li et al., "Clinical implication of coronary tortuosity in patients with coronary artery disease," *PLoS One*, vol. 6, no. 8, Aug. 2011, Art. no. e24232.
- [51] J. Saw et al., "Nonatherosclerotic coronary artery disease in young women," *Can. J. Cardiol.*, vol. 30, no. 7, pp. 814–819, 2014.
- [52] H. J. Carpenter et al., "A review on the biomechanics of coronary arteries," *Int. J. Eng. Sci.*, vol. 147, 2020, Art. no. 103201.
- [53] A. Candreva et al., "Is spontaneous coronary artery dissection (SCAD) related to local anatomy and hemodynamics? An exploratory study," *Int. J. Cardiol.*, vol. 386, pp. 1–7, 2023.
- [54] P. Tajik et al., "Asymmetrical distribution of atherosclerosis in the carotid artery: Identical patterns across age, race, and gender," *Eur. J. Prev. Cardiol.*, vol. 19, no. 4, pp. 687–697, 2012.
- [55] R. Chaudhary et al., "Gender differences in thrombogenicity among patients with angina and non-obstructive coronary artery disease," *J. Thromb. Thrombolysis*, vol. 48, pp. 373–381, 2019.
- [56] L. Pilote et al., "A comprehensive view of sex-specific issues related to cardiovascular disease," *Can. Med. Assoc. J.*, vol. 176, no. 6, pp. S1–S44, 2007.
- [57] A. Kumar et al., "Low coronary wall shear stress is associated with severe endothelial dysfunction in patients with nonobstructive coronary artery disease," *Joint Autom. Control Conf.: Cardiovasc. Interv.*, vol. 11, no. 20, pp. 2072–2080, 2018.
- [58] F. D. Kolodgie et al., "Is pathologic intimal thickening the key to understanding early plaque progression in human atherosclerotic disease?," *Arteriosclerosis, Thromb., Vasc. Biol.*, vol. 27, pp. 986–989, 2007.
- [59] K. S. Cunningham and A. I. Gotlieb, "The role of shear stress in the pathogenesis of atherosclerosis," *Lab. Investigation*, vol. 85, no. 1, pp. 9–23, 2005.
- [60] J.-A. Eastwood and L. V. Doering, "Gender differences in coronary artery disease," *J. Cardiovasc. Nurs.*, vol. 20, no. 5, pp. 340–351, 2005.
- [61] A. H. E. M. Maas and Y. E. A. Appelman, "Gender differences in coronary heart disease," *Netherlands Heart J.*, vol. 18, no. 12, pp. 598–603, 2010.
- [62] A. R. Pries, D. Neuhaus, and P. Gaetgens, "Blood viscosity in tube flow: Dependence on diameter and hematocrit," *Amer. J. Physiol.-Heart Circulatory Physiol.*, vol. 263, no. 6, pp. H1770–H1778, 1992.